Role of Arginine 439 in Substrate Binding of 5-Aminolevulinate Synthase†

Dongwei Tan, Tracy Harrison, Gregory A. Hunter, and Gloria C. Ferreira*

Department of Biochemistry and Molecular Biology, College of Medicine, Institute for Biomolecular Science, H. Lee Moffitt Cancer Center and Research Institute, University of South Florida, Tampa, Florida 33612

Received August 5, 1997; Revised Manuscript Received November 14, 1997

ABSTRACT: 5-Aminolevulinate synthase (EC 2.3.1.37) catalyzes the first reaction in the heme biosynthetic pathway in nonplant eukaryotes and some prokaryotes. Homology sequence modeling between 5-aminolevulinate synthase and some other α-family pyridoxal 5′-phosphate-dependent enzymes indicated that the residue corresponding to the Arg-439 of murine erythroid 5-aminolevulinate synthase is a conserved residue in this family of pyridoxal 5′-phosphate-dependent enzymes. Further, this conserved arginine residue in several enzymes, e.g., aspartate aminotransferase, for which the three-dimensional structure is known, has been shown to interact with the substrate carboxyl group. To test whether Arg-439 is involved in substrate binding in murine erythroid 5-aminolevulinate synthase, Arg-439 and Arg-433 of murine erythroid 5-aminolevulinate synthase were each replaced by Lys and Leu using site-directed mutagenesis. The R439K mutant retained 77% of the wild-type activity; its K_m values for both substrates increased 9−13-fold, while the activity of R433K increased 2-fold and the K_m values for both substrates remained unchanged. R439L had no measurable activity as determined using a standard 5-aminolevulinate synthase enzyme-coupled activity assay. In contrast, the kinetic parameters for R433L were comparable to those of the wild-type. Dissociation constants (K_d) for glycine increased 5-fold for R439K and at least 30-fold for R439L, while K_d values for glycine for both R433K and R433L mutants were similar to those of the wild-type. However, there was not much difference in methylamine binding among the mutants and the wild-type, excepting of a 10-fold increase in $K_d^{methylamine}$ for R439L. R439K proved much less thermostable than the wild-type enzyme, with the thermotransition temperature, $T_{1/2}$, determined to be 8.3 °C lower than that of the wild-type enzyme. In addition, *in vivo* complementation analysis demonstrated that in the active site of murine erythroid 5-aminolevulinate synthase, R439 is contributed from the same subunit as K313 (which is involved in the Schiff base linkage of the pyridoxal 5′-phosphate cofactor) and D279 (which interacts electrostatically with the ring nitrogen of the cofactor), while another subunit provides R149. Taken together, these findings suggest that Arg-439 plays an important role in substrate binding of murine erythroid 5-aminolevulinate synthase.

5-Aminolevulinate synthase (ALAS,[1] EC 2.3.1.37) is the first enzyme in the heme biosynthetic pathway in nonplant eukaryotes and some prokaryotes (*1, 2*). It catalyzes the condensation of glycine and succinyl-CoA to produce 5-aminolevulinate (ALA), coenzyme A, and CO_2. In animals, there are two different ALAS isoforms encoded by two separate genes, the housekeeping form and the erythroid-specific form (*3*). ALAS functions as a homodimer and requires pyridoxal 5′-phosphate (PLP) as an essential cofactor. The ALAS active site resides at the subunit interface and contains catalytically essential residues from two subunits (*4*).

Although the amino acid sequences for all known ALASs, ranging from bacteria to human, exhibit a high degree of homology, no significant identity has been found with other PLP-dependent enzymes (*2*). In fact, of the over 300 PLP-dependent enzyme sequences known, many have no detectable sequence identity. However, despite the low sequence similarity, Mehta et al. (*5*), using hydropathy plots, secondary structure predictions, and profile analysis, succeeded in classifying 51 sequences of 14 different aminotransferases into four different subfamilies (in each subfamily, the enzymes are closely related). Interestingly, the alignment of three of the subfamilies indicated only four (out of approximately 400) invariant residues (*5*). When this type of survey was extended to all known PLP-dependent enzyme sequences, ALAS was placed in the α subfamily, which contains aspartate aminotransferase (AAT) and enzymes which catalyze primarily $C^α$ stereoselectivity reactions (*6*). More recently, Grishin et al. (*7*), using similarities in sequence, secondary structure, hydrophobicity profiles, and structural similarities with enzymes of known structure, classified the sequenced PLP-dependent enzymes into seven fold types (i.e., fold I−VII). ALAS was predicted to possess the same fold as that of AAT (i.e., fold I). In addition, the

† This work was supported by the National Institutes of Health (Grant DK52053). T.H. is a recipient of an Institute for Biomolecular Science−Woods Undergraduate Research Fellowship, University of South Florida. G.A.H. is an American Heart Association Predoctoral Fellow, Florida Division (9504006). G.C.F. is a recipient of a NSF Young Investigator Award (MCB-9257656).

* Author to whom correspondence should be addressed. Telephone: (813) 974-5797. Fax: (813) 974-5798. E-mail: gferreir@com1.med.usf.edu.

[1] Abbreviations: ALA, 5-aminolevulinate; ALAS, 5-aminolevulinate synthase; PLP, pyridoxal 5′-phosphate; SDS, sodium dodecyl sulfate; SDS−PAGE, SDS−polyacrylamide gel electrophoresis.

S0006-2960(97)01928-4 CCC: $15.00
Published on Web 01/22/1998

availability of AAT high-resolution crystal structures and a solid knowledge of the functions of several active site residues make AAT a good homology model for ALAS.

An arginine residue (Arg-386 in pig cytosolic AAT) was identified as one of four invariant residues in all aminotransferases (*5*). Arg-386 binds the α-carboxylate group of the substrate and determines to a large extent the orientation of the substrate moiety relative to the plane of the cofactor−substrate imine (*8*). Further, this Arg residue has been replaced by a Lys, Tyr, or Phe residue (*8*, *9*). All of the AAT mutants showed dramatically reduced enzymatic activity, and even the Lys residue proved an inadequate substitute (10^2-10^3-fold decrease in k_{cat}).

Arg-439 of murine erythroid ALAS appears to be a conserved residue in all ALASs and to correspond to the invariant Arg residue in aminotransferases (i.e., Arg-386 in pig cytosolic AAT). To determine whether Arg-439 in murine erythroid ALAS has a functional role similar to that of AAT Arg-386, we constructed several ALAS variants in which Arg-439 and the adjacent Arg-433 were independently mutated and investigated the catalytic and substrate-binding properties of the mutated variants in relation to those of the wild-type ALAS. Results of the present study indicate that Arg-439 plays a critical role in substrate binding of murine erythroid ALAS. In addition, *in vivo* complementation studies were used to establish the architecture of the ALAS active site by defining the position of Arg-439 in relation to other essential residues (i.e., Arg-149, Asp-279, and Lys-313).

EXPERIMENTAL PROCEDURES

Materials

Restriction enzymes and T4 DNA ligase were obtained from New England Biolabs and were used according to the supplier's instructions. The GeneClean II kit was a product of Bio 101 Inc. The Chameleon mutagenesis kit was from Stratagene. Acrylamide and gel reagents were purchased from Bio-Rad. Sequenase and the sequencing kit were from U.S. Biochemical Corp. [α-^{35}S]dATP was from Dupont/NEN Research Products. The bicinchoninic acid protein assay reagents were obtained from Pierce Chemical Co. Ni-NTA agarose was purchased from Qiagen. Oligonucleotide primers were synthesized by Cybersyn. All other chemicals were of the highest purity available. The *Escherichia coli* strain HU227 (*10*) was a gift from Dr. C. S. Russell (City University of New York).

Methods

Mutagenesis, Expression, and Purification of R439K, R439L, R433K, and R433L. Plasmid pDT6, which contains a full-length mouse erythroid ALAS wild-type sequence with an N-terminal extension consisting of five histidine residues (*4*), was purified from its *E. coli* DH5α host cell. Single-stranded DNA of this plasmid was prepared according to the alkaline lysis method (*11*). Site-directed mutagenesis was performed on the single-stranded DNA using the Chameleon mutagenesis kit from Stratagene. The mutagenic oligonucleotides for R439K, R439L, R433K, and R433L were 5′-AGC TAC TGA AGT TGG CCC C-3′, 5′-GAG CTA CTG CTC TTG GCC CCC-3′, 5′-CTG TGC CTA AAG GTG AGG A-3′, and 5′-CCA ACT GTG CCT CTT GGT GAG GAG C-3′, respectively. Clones obtained after the mutagenesis procedure were screened using DNA sequencing, as described in the dideoxynucleotide chain termination method (*12*). The resulting expression plasmids containing the mutation R439K, R439L, R433K, or R433L were named pDT12, pDT13, pDT11, and pDT9, respectively. The mutant and wild-type enzymes were overproduced in *E. coli* DH5α host strain harboring the different expression plasmids and purified to homogeneity using nickel chelate agarose chromatography, as previously described for the wild-type enzyme (*4*) except for one modification. Briefly, the histidine-tagged protein was eluted with 200 mM imidazole buffer, pH 7.2, containing 20 mM PLP, 5 mM β-mercaptoethanol, and 10% glycerol. Subsequently, the fractions containing ALAS were precipitated with 50% (w/v) poly(ethylene glycol) and resuspended in 20 mM imidazole buffer, pH 7.2, containing 20 mM PLP, 5 mM β-mercaptoethanol, and 10% glycerol.

SDS−PAGE, Protein Concentration Determination, UV−Visible Spectra, and Kinetic Studies. SDS−PAGE and protein concentration determination were performed as described previously in Tan and Ferreira (*4*). Briefly, 15% acrylamide and 1.5-mm thick gels were used in SDS−PAGE, and the protein concentrations were determined by the bicinchoninic acid assay according to the manufacturer's instructions. A Shimadzu UV2100U spectrophotometer was used to measure the UV−visible absorption spectra of the wild-type and mutant ALASs. A continuous spectrophotometric assay was used to measure ALAS enzyme activity (*13*) with a modification of temperature to 37 °C. Hanes and secondary plots were employed to obtain k_{cat} and K_m values, which were determined for glycine and succinyl-CoA at constant concentrations of 1−72 μM for succinyl-CoA and 10−400 mM for glycine, respectively.

Determination of Dissociation Constants (K_d) of Glycine and Methylamine. The K_d values were determined by UV−visible spectrometric titration of ALAS with glycine or methylamine. ALAS wild-type and the mutant proteins were taken in 20 mM imidazole buffer containing 5 mM β-mercaptoethanol and 25% glycerol at a concentration range of 6−12 μM. High concentrations of glycine (2 M) and methylamine (1 M) were used in the experiments to ensure minimum dilution of the ALAS samples. UV−visible spectra were recorded from 250 to 600 nm after each addition of glycine or methylamine. The binding of glycine or methylamine was monitored by an absorbance increase at 410 nm, and the increases were used to calculate the K_d values. K_d for glycine is defined as

$$K_d = ([Gly][ALAS])/[Gly\text{-}ALAS] \quad (1)$$

where [Gly] and [ALAS] are the concentrations of free glycine and ALAS, respectively, and [Gly-ALAS] represents the concentration of the glycine-bound ALAS. Further, K_d was calculated using the formula

$$[Gly]_t/\Delta Abs_{410} = [Gly]_t/\Delta Abs_{max} + K_d/\Delta Abs_{max} \quad (2)$$

where ΔAbs_{410} is the absorption increase at 410 nm and $[Gly]_t$ is the total glycine concentration. ΔAbs_{410} was plotted

	433								439			
Mouse erythroid	T	V	P	**R**	G	E	E	L	L	**R**	L	A	P
Human housekeeping	T	V	P	**R**	G	E	E	L	L	**R**	I	A	P
Human erythroid	T	V	P	**R**	G	E	E	L	L	**R**	L	A	P
Rat housekeeping	T	V	P	**R**	G	E	E	L	L	**R**	I	A	P
Rat erythroid	T	V	P	**R**	G	E	E	I	L	**R**	L	A	P
Chicken housekeeping	T	V	P	**R**	G	E	E	L	L	**R**	I	A	P
Chicken erythroid	T	V	P	**R**	G	Q	E	L	L	**R**	I	A	P
Saccharomyces cerevisiae hem1	T	V	A	**R**	G	T	E	R	L	**R**	I	T	P
Aspergillus nidulans	T	V	P	**R**	G	E	E	R	L	**R**	I	T	P
Paracocus denitrificans	T	V	P	**R**	G	T	E	R	L	**R**	F	T	A
Rhodobacter spheroides hemT	T	V	A	**R**	G	Q	E	R	F	**R**	L	T	P
Rhodobacter spheroides hemA	T	V	P	**R**	G	T	E	R	L	**R**	F	T	P
Rhodobacter capsulatus	T	V	P	**R**	G	T	E	R	L	**R**	F	T	P
Agrobacterium radiobacter	T	V	P	**R**	K	T	E	R	L	**R**	I	T	P
Bradyrhizobium japonicum	T	V	A	**K**	G	S	E	R	L	**R**	I	T	P

FIGURE 1: Alignment of all known ALAS sequences around murine erythroid ALAS Arg-433 and Arg-439 residues. Nonhomologous amino acids are underlined [adapted from Ferreira and Gong (*2*)].

against $[Gly]_t$ and ΔAbs_{max}(maximum absorbance increase at 410 nm), and K_d was calculated by a linear curve fit of the experimental data using the *Slide* program (Advanced Graphic Software, Inc.). Similar K_d definition and calculation were also applied to methylamine.

Determination of the Thermostability of ALAS Wild-type and Mutants. The ALAS sample at a protein concentration of 5 μM was incubated at a given temperature for 3 min, and then cooled to 0 °C, using an MJ Research MiniCycler. Activity assays were performed on the treated sample at 37 °C with 24 μM succinyl-CoA and 150 mM glycine for the wild-type and R433K and R433L mutants, and 72 μM succinyl-CoA and 400 mM glycine for the R439K mutant. The enzymatic activity from the sample treated at 0 °C was set as 100%. The thermotransition temperature, $T_{1/2}$, is defined as the temperature needed for a 50% loss of activity.

Construction of Plasmid pJGR149Ac and Cotransformation of E. coli HU227 Cells. The pJGR149Ac plasmid was constructed from pJGR149A and pDT4 (i.e., R149A and K313A expression plasmids, respectively, see ref *4*) and contains a full-length mouse erythroid ALAS R149A mutant. A DNA fragment encoding the full-length R149A ALAS mutant was retrieved from pJGR149A (*14*) upon digestion with *Sal*I and *Bam*HI. The fragment was then ligated into pDT4, which was previously digested with *Sal*I and *Bam*HI. This ligation yielded the R149A ALAS mutant overexpression plasmid with a chloramphenicol resistance gene. *E. coli* HU227 cells, transformed with pJGR149Ac or pDT4, were grown in LB medium (*11*) containing 35 mg/mL chloramphenicol and 10 mg/mL ALA. HU227 cells, cotransformed with pJGR149Ac (or pDT4) and D279A, R439L expression plasmids, or ALAS wild-type overexpression plasmid (pDT6), were grown in LB medium containing 50 mg/mL ampicillin and 35 mg/mL chloramphenicol, with or without 10 mg/mL ALA, respectively.

RESULTS

Alignment of All Known ALAS Sequences around Murine Erythroid ALAS Arg-439. Protein sequence alignment of all known ALASs indicated that murine erythroid ALAS Arg-439 is an invariant residue (Figure 1). Further, sequence comparison of the murine erythroid ALAS with the pig cytosolic AAT reveals that the erythroid ALAS Arg-439 might correspond to the AAT Arg-386, which was previously shown to be one of the four invariant residues in aminotransferases (*5*) and to be involved in substrate binding (*8*). Another conserved Arg residue (R433) is located just six amino acids upstream of Arg-439, with the exception of *Bradyhizobium japonicum* ALAS in which this position contains a Lys residue. To determine whether one of the two Arg residues is critical to the substrate binding in ALAS, both R439 and R433 were replaced by Lys and Leu using site-directed mutagenesis.

Kinetic Studies of ALAS R439 and R433 Mutants. Kinetic parameters were determined for the purified R439- and R433-directed mutants (Table 1). For the Arg-to-Leu mutations, no measurable activity was detected in R439L, whereas the kinetic parameters of R433L were comparable to the values of the wild-type enzyme. For the Arg-to-Lys mutations, the activity of R439K mutant decreased to 77% of that of the wild-type, while K_m values for both substrates increased 9−13-fold; the activity of R433K mutant increased 2-fold, while K_m values for both substrates remained close to those of the wild-type enzyme.

UV−Visible Spectroscopic Properties. R439K, R439L, R433K, R433L, and the wild-type ALASs all exhibited similar UV−visible absorption spectra (Figure 2 and inset). Absorption maxima at 330 and 410 nm are characteristic of different ionization states of the internal aldimine bond between the PLP and the ALAS (either wild-type or mutants). The two absorption maxima (at 330 and 410 nm) correspond to the unprotonated and protonated forms, respectively.

Affinity Constant for Binding of Glycine or Methylamine to the Wild-Type and Mutant Forms of ALAS. The binding of glycine or methylamine can be monitored spectrophotometrically by an increase in absorbance at 410 nm, which allows the determination of the dissociation constants (K_d) by titrating the enzyme with glycine or methylamine. The obtained K_d values of the mutants and the wild-type are summarized in Table 2. K_d for glycine increased 5-fold for R439K, while no absorption change at 410 nm was observed in R439L using up to a 200 mM glycine concentration in titration. In contrast, for the R433 mutants the K_d values remained close to that of the wild-type. There was no significant difference among the K_d values for methylamine for the mutants and the wild-type with the exception of R439L. K_d for glycine for the mutants and the wild-type

Table 1: Kinetic Parameters for R439 and R433 Mutants of ALAS

	K_m^{Gly} (mM)	$K_m^{Suc-CoA}$ (μM)	V_{max} (nmol mg^{-1} h^{-1})	k_{cat} (min^{-1})	k_{cat}/K_m^{Gly} (mM^{-1} min^{-1})	$k_{cat}/K_m^{Suc-CoA}$ (μM^{-1} min^{-1})
wild-type	11.7	2.03	4.23×10^4	39.5	3.38	19.5
R439L			0	0		
R439K	103	27.3	3.26×10^4	30.5	0.296	1.11
R433L	18.4	3.24	5.41×10^4	50.5	2.74	15.6
R433K	14.5	2.24	8.66×10^4	80.9	5.58	36.1

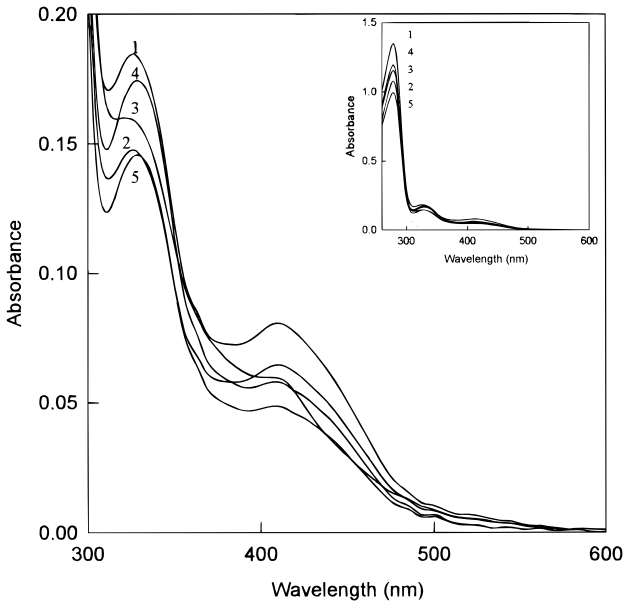

FIGURE 2: UV−visible absorption spectra of ALAS R433 and R439 mutants. UV−visible absorption spectra were recorded in 20 mM imidazole buffer, pH 7.2. Curves: 1, wild-type (23.4 μM); 2, R439L (18.7 μM); 3, R439K (20.0 μM); 4, R433L (20.8 μM); 5, R433K (17.3 μM). (Inset) Absorption spectra of ALAS wild-type and mutants in the 260−600 nm range.

were also measured at different pH values. The results are illustrated in Figure 3 and indicate that higher pH values cause stronger glycine binding by ALAS. For the R439L mutant, no absorption change at 410 nm could be observed using up to a 200 mM glycine concentration at all given pH values.

Thermostability Characterization of Active Arginine Mutants. Thermostability experiments were conducted to measure the relative stability of ALAS wild-type, R439K, R433K, and R433L mutant enzymes. Activity as a function of temperature is shown in Figure 4, in which the thermotransition temperature, $T_{1/2}$, is defined as the temperature needed for a 50% activity loss. $T_{1/2}$ was 47, 52.8, 54.1, and 55.3 °C for R439K, R433K, R433L, and the wild-type, respectively.

Localization of R439 and D279 in the ALAS Active Site. *In vivo* complementation studies were used to demonstrate that the ALAS active site is located at the subunit interface and contains catalytically essential residues R149 (which cannot be replaced by other amino acid residues) and K313 (which is involved in the Schiff base linkage of the PLP cofactor) from the two subunits (*4*). To localize the presently identified substrate-binding R439 residue in the shared active site with respect to Arg-149, Lys-313, and another important residue (i.e., D279), which recently was found to be critical to ALAS enzymatic activity (unpublished results), *in vivo* complementation studies were performed. Specifically, according to the intersubunit active site arrangement of ALAS, if two different inactive mutants (each with a single mutation of an active site residue) can complement each other and restore ALAS activity, then the two active site residues should reside in different subunits of the dimer. *hemA*$^-$ HU227 cells can grow only in a medium supplemented with ALA or when transformed with a functional ALAS-encoding plasmid, and therefore these cells were used to examine the restoration of ALAS activity with the *in vivo* complement experiments. After the cotransformation of two inactive ALAS mutant plasmids, the rescue of HU227 cell growth in a non-ALA supplemented medium indicated the production of an active ALAS. The cotransformation results are summarized in Table 3, indicating that in the ALAS active site R439 is contributed from the same subunit as K313 and D279, while the other subunit provides R149.

DISCUSSION

ALAS was recently classified in fold type I of the PLP-dependent enzymes (*7*). This fold type includes four classes of aminotransferases with AAT as one of the members of class I. Among the PLP-dependent enzymes, AAT is probably the most extensively studied enzyme. Since high-resolution crystal structures and the functions of many of the active site residues are known for AAT, sequence alignments of AAT and other aminotransferases have been used to propose the function(s) of an amino acid residue in a specific aminotransferase (*15*−*19*). Significantly, only four out of a total of about 400 amino acid residues have proved invariant in the aligned aminotransferase sequences (*5*). AAT is particularly suitable for homology modeling of ALAS, given that both ALAS and AAT belong to the same predicted PLP-dependent enzyme fold type group.

In AAT, Arg-386 interacts with the α-carboxylate group of the substrate. Replacement of this residue with tyrosine or phenylalanine results in a 10^5-fold decrease in the catalytic efficiency of AAT (*9*). Even the conservative replacement of a lysine residue at this position can retain only about 0.8% of the activity of the wild-type, suggesting that both size and shape of a positively charged arginine residue at position 386 are essential for efficient catalysis by AAT. Using protein sequence alignment, we proposed that Arg-439 of murine erythroid ALAS forms a salt bridge with the α-carboxylate group of substrate glycine. To assess this hypothesis, we prepared and studied the mutants R439K and R439L. In addition, substitution of another conservative arginine residue Arg-433 with Lys and Leu was used as a control. The R439K mutation resulted in a slightly decreased k_{cat} and 9−13-fold increases in the K_m values for both glycine and succinyl-CoA substrates. Interestingly, k_{cat} of the R433K mutant increased 2-fold, while the K_m values for both substrates remained close to those of the wild-type. The removal of the positive charge proved fatal to ALAS, as evidenced by the undetectable enzymatic activity in the R439L mutant. In contrast, for R433L the kinetic parameters were still comparable to the values of the wild-type enzyme. Dissociation constants (K_d) of glycine (NH_2CH_2COOH) and methylamine (CH_3NH_2) were also measured for the mutants and the wild-type. Here methylamine could be viewed as a glycine molecule without the α-carboxylate group and in theory should result in similar binding affinity among all the mutants. Binding of glycine exhibited a 5-fold decrease in R439K and was extremely difficult in R439L, while K_ds for glycine for R433K and R433L remained similar to that of the wild-type. However, there was not much difference in methylamine affinity among the mutants and the wild-type with the exception of a 10-fold increase in $K_d^{methylamine}$ for R439L, probably due to a conformational change induced by the mutation. However, the R439L mutant still forms a dimer and remains most of the structural integrity of the wild-

Table 2: Glycine and Methylamine Dissociation Constants for ALAS Wild-Type and R439 and R433 Mutants

	R439L	R439K	R433L	R433K	wild-type
K_d^{Gly} (mM)	≫200	33.0 (1.95[a])	5.74 (0.51)	7.25 (0.67)	6.76 (0.59)
$K_d^{methylamine}$ (mM)	157 (9.1)	12.2 (0.92)	13.1 (1.13)	10.1 (1.08)	12.6 (0.96)

[a] Standard errors.

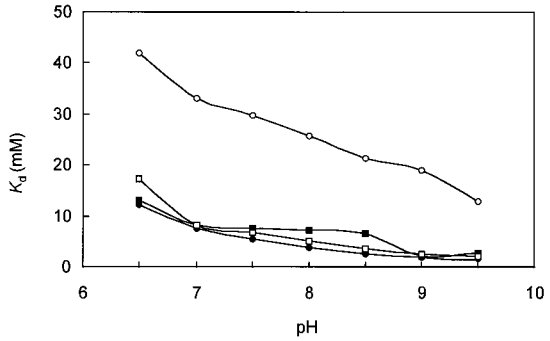

FIGURE 3: pH dependence of glycine binding of ALAS R433 and R439 mutants. Glycine dissociation constants of wild-type and R433K, R433L, and R439K mutants were measured at pH 6.5−9.5. Glycine (2M) was used in the experiments to ensure minimum dilution of the samples. The pH was adjusted by adding acetic acid or NaOH into the buffer containing 20 mM imidazole and 20 mM AMPSO: □, wild-type; ○, R439K; ●, R433L; ■, R433K.

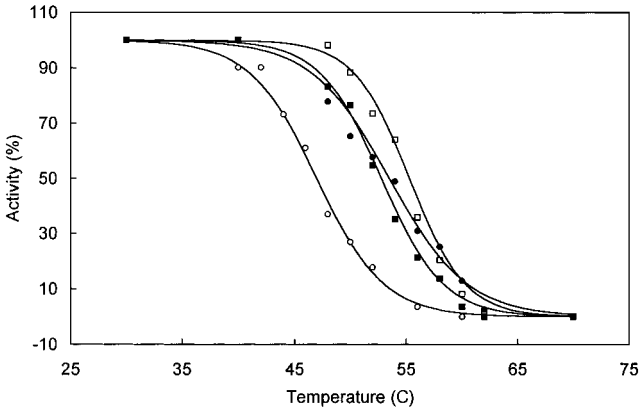

FIGURE 4: Thermostability of ALAS wild-type and arginine mutant enzymes. ALAS samples were incubated at a given temperature for 3 min, and then cooled to 0 °C, upon which activity assays were performed. The enzymatic activity from the sample treated at 0 °C was set as 100%: □, wild-type; ○, R439K; ●, R433L; ■, R433K. The thermotransition temperature, $T_{1/2}$, is defined as the temperature needed for a 50% activity loss. $T_{1/2}$ was 47, 52.8, 54.1, and 55.3 °C for R439K, R433K, R433L, and the wild-type, respectively.

type enzyme, as indicated by the gel filtration and far-UV CD experiments, respectively (data not shown). Taken together, all these results suggest that a positively charged group at position 439 is necessary and sufficient for glycine binding and efficient catalysis by ALAS. Further, the binding affinity of glycine for R439K, R433K, R433L, and the wild-type was investigated at pH values 6.5−9.5. Similar results were obtained for the mutants and the wild-type; higher pH resulted in stronger glycine binding by ALAS. Since the deprotonated form of glycine binds the Schiff base protonated form in the substrate binding mechanism (Gly + $EH^+ \leftrightarrow E{\cdot}GlyH^+$), one possible interpretation is that the improved binding affinity of glycine is caused by a combination of the increased amount of the deprotonated form of glycine and the decreased amount of the Schiff base protonated form when pH is changed from a low value to a high value. Mutations of the arginines also affect enzyme stability, as evidenced by the thermostability experiments (Figure 4). All of the mutants were less stable than the wild-type. Interestingly, a Lys residue proved an adequate substitute for R439 in enzymatic catalysis. However, the R439K mutant is much more vulnerable to heat than the wild-type, suggesting that R439 may play an important role in ALAS stability.

Previous studies showed that ALAS functions as a homodimer with two shared active sites containing catalytically essential residues (e.g., R149 and K313) from each of the two subunits (*4*). The availability of other important residues allowed us to extend the active site map. The capability of R439A and D279A to recover ALAS enzymatic activity when cotransformed with R149A, but not K313A in *hemA*$^-$ HU227 cells, suggests that each of these residues is contributed to the active site from the same subunit as Lys-313 (Figure 5).

Most of the PLP-dependent enzymes can be assigned to one of three different subfamilies of homologous proteins, based on the position of the carbon atom of the substrate at which covalency changes take place (*6*). ALAS was categorized in the α subfamily, in which enzymes catalyze primarily C^α stereoselective reactions (*6*). Different reaction types in the α subfamily result from different C^α bond cleavages after conversion of internal to external aldimine (Scheme 1, modified from ref *20*). Although the Arg residue critical for substrate binding was found to be invariant in sequence alignments of aminotransferases and many other PLP-dependent enzymes, few enzymes have been investigated in terms of this important residue. Besides AAT and ALAS, only 1-aminocyclopropane-1-carboxylate synthase (ACC synthase) has been studied regarding to the Arg residue (Arg-407 in ACC synthase) involved in substrate binding (*16*). ALAS can be classified in the same transamination type as AAT since the first step in ALAS catalysis involves the removal of H^+ from C^α (*21*−*23*), while ACC synthase can be categorized in the R group cleavage type (*16*). For AAT and ACC synthase, substitution of the arginine residue even with lysine resulted in a substantial drop in k_{cat} values, suggesting the amino acid at this position must be arginine (*8*, *16*). Both size and shape of the positive charge are essential for efficient catalysis. However, the ALAS R439K mutant still retained 77% of the wild-type activity, suggesting that a positively charged group at position 439 is sufficient for substrate binding and efficient catalysis by ALAS. Apparently, the significant difference in the enzymatic activity of the lysine mutant between ALAS and the other two enzymes results from their different reaction mechanisms. Specifically, X-ray crystallographic studies of AAT reveal that the substrate−coenzyme complex is held tightly within the active site by interaction with multiple amino acid side chains including Arg-386 (*24*). A stable bond between the α-carboxylate group of the substrate and the side chain of Arg-386 ensures a correct alignment of the substrate within

Table 3: HU227 Transformation by Different Plasmids

mutant plasmid(s)	medium	growth	medium	growth
D279A	LB + Amp[a] + Cm[b]	−	LB + Amp + Cm + ALA	−
R439L	LB + Amp + Cm	−	LB + Amp + Cm + ALA	−
R149A	LB + Amp + Cm	−	LB + Amp + Cm + ALA	−
R149A+D279A	LB + Amp + Cm	+	LB + Amp + Cm + ALA	+
R149A+K313A	LB + Amp + Cm	+	LB + Amp + Cm + ALA	+
R149A+R439L	LB + Amp + Cm	+	LB + Amp + Cm + ALA	+
R149A+WT[c]	LB + Amp + Cm	+	LB + Amp + Cm + ALA	+
K313A	LB + Amp + Cm	−	LB + Amp + Cm + ALA	−
K313A+R149A	LB + Amp + Cm	+	LB + Amp + Cm + ALA	+
K313A+D279A	LB + Amp + Cm	−	LB + Amp + Cm + ALA	+
K313A+R439L	LB + Amp + Cm	−	LB + Amp + Cm + ALA	+
K313A+WT	LB + Amp + Cm	+	LB + Amp + Cm + ALA	+

[a] Amp, ampicillin. [b] Cm, chloramphenicol. [c] WT, wild-type ALAS.

Scheme 1

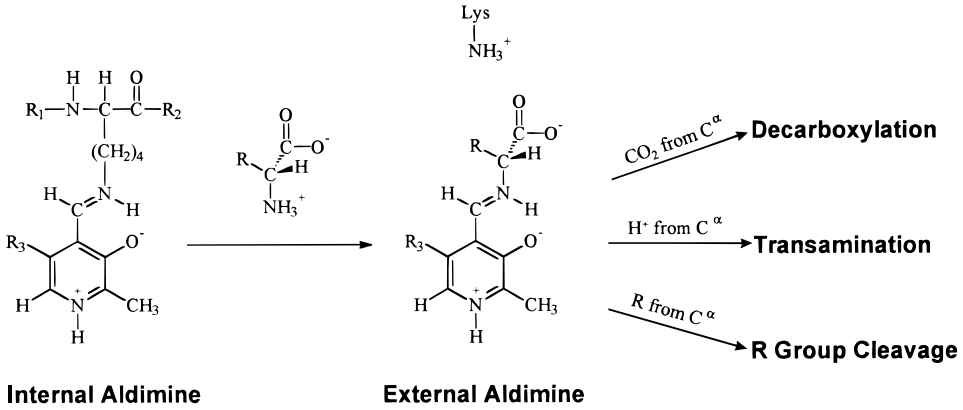

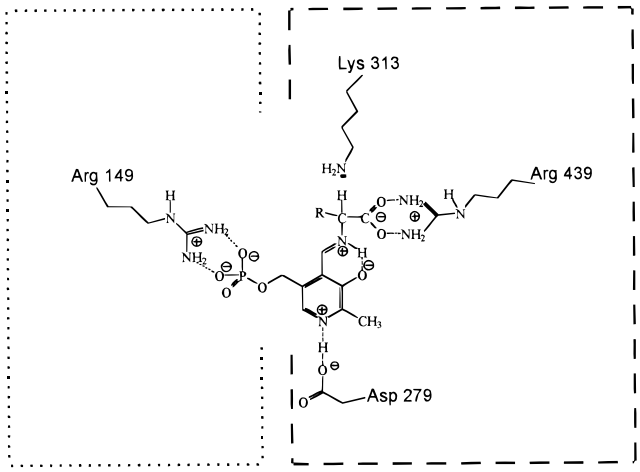

FIGURE 5: Schematic representation of the putative ALAS intersubunit active site arrangement. Amino acid residues potentially contributing to the intersubunit active site of ALAS are shown with respect to R149 and K313 residues.

the active site during the entire catalysis (*8*). A similar mechanism may also exist in ACC synthase (*16*). However, for ALAS the α-carboxylate group of substrate glycine is eliminated from Cα after the addition of the second substrate succinyl CoA to the enzyme−substrate complex (*25*−*27*). Interaction between Arg-439 and the α-carboxylate group of glycine can be interpreted as being utilized only for the initial substrate binding but not being responsible for the holding of the substrate−coenzyme conjugate during the entire catalysis. Therefore, the positively charged group of the side chain of a Lys residue is sufficient for this substrate binding function.

In summary, by using site-directed mutagenesis and kinetic studies, we provide conclusive evidence that R439 in murine erythroid ALAS plays an important role in substrate binding. In addition, *in vivo* complementation analysis demonstrates that R439 and the other important residue D279 are contributed from the same subunit as K313 in the shared active site of ALAS.

ACKNOWLEDGMENT

We thank Dr. J. Gong in our laboratory for providing the D279A mutant plasmid.

REFERENCES

1. Jordan, P. M. (1991) in *Biosynthesis of Tetrapyrroles* (Jordan, P. M., Ed.) pp 1−66, Elsevier, Amsterdam.
2. Ferreira, G. C., and Gong, J. (1995) *J. Bioenerg. Biomembr. 27*, 151−159.
3. Riddle, R. D., Yamamoto, M., and Engel, J. E. (1989) *Proc. Natl. Acad. Sci. U.S.A. 86*, 792−796.
4. Tan, D., and Ferreira, G. C. (1996) *Biochemistry 35*, 8934−8941.
5. Mehta, P. S., Hale, T. I., and Christen, P. (1993) *Eur. J. Biochem. 214*, 549−561.
6. Alexander, F. W., Sandmeier, E., Mehta, P. K., and Christen, P. (1994) *Eur. J. Biochem. 219*, 953−960.
7. Grishin, N. V., Phillips, M. A., and Goldsmith, E. J. (1995) *Protein Sci. 4*, 1291−1304.
8. Inoue, Y., Kuramitsu, S., Inoue, K., Kagamiyama, H., Hiromi, K., Tanase, S., and Morino, Y. (1989) *J. Biol. Chem. 264*, 9673−9681.
9. Danishefsky, A. T., Onnufer, J. J., Petsko, G. A., and Ringe, D. (1991) *Biochemistry 30*, 1980−1985.
10. Li, J.-M., Brathwaite, O., Cosloy, S., and Russell, C. S. (1989) *J. Bacteriol. 171*, 2547−2552.

11. Sambrook, J., Frisch, E. F., and Maniatis, T. (1989) *Molecular Cloning: A Laboratory Manual*, 2nd ed., Cold Spring Harbor Laboratory, Cold Spring Harbor, NY.
12. Sanger, F., Nicklen, S., and Coulson, A. R. (1977) *Proc. Natl. Acad. Sci. U.S.A. 74*, 5463−5467.
13. Hunter, G. A., and Ferreira, G. C. (1995) *Anal. Biochem. 226*, 221−224.
14. Gong, J., and Ferreira, G. C. (1995) *Biochemistry 34*, 1678−1685.
15. Pascarella, S., Schirch, V., and Bossa, F. (1993) *FEBS Lett. 331*, 145−149.
16. White, M. F., Vasquez, J., Tang, S. F., and Kirsch, J. F. (1994) *Proc. Natl. Acad. Sci. U.S.A. 91*, 12428−12432.
17. Chen, H. Y., Demidkina, T. V., and Phillips, R. S. (1995) *Biochemistry 34*, 12276−12283.
18. Momany, C., Ghosh, R., and Hackert, M. L. (1995) *Protein Sci. 4*, 849−854.
19. Osterman, A. L., Kinch, L. N., Grishin, N. V., and Phillips, M. A. (1995) *J. Biol. Chem. 270*, 11797−11802.
20. Smith, D. M., Thomas, N. R., and Gani, D. (1991) *Experientia 47*, 1104−1117.
21. Akhtar, M., and Jordan, P. M. (1968) *J. Chem. Soc., Chem. Commun.* 1691−1692.
22. Zaman, Z., Jordan, P. M., and Akhtar, M. (1973) *Biochem. J. 135*, 257−263.
23. Laghai, A., and Jordan, P. M. (1976) *Biochem. Soc. Trans. 4*, 52−53.
24. Arnone, A., Rogers, P. H., Hyde, C. C., briley, P. D., Metzler, C. M., and Metzler, D. E. (1985) in *Transaminases* (Christen, P., and Metzler, D. E., Eds.) pp 138−155, John Wiley & Sons, New York.
25. Abboud, M. M., Jordan, P. M., and Akhtar, M. (1974) *J. Chem. Soc., Chem. Commun.*, 643−644.
26. Laghai, A., and Jordan, P. M. (1977) *Biochem. Soc. Trans. 5*, 299−301.
27. Emery, V., and Akhtar, M. (1987) in *Enzyme Mechanisms* (Page, M. I., and Williams, A., Eds.) pp 345−389, The Royal Society of Chemistry, Letchworth, U.K.

BI971928F